EPJ Web of Conferences will be set by the publisher
DOI: will be set by the publisher
© Owned by the authors, published by EDP Sciences, 2015

Performance Studies of Micromegas Chambers for the New Small Wheel Upgrade Project

S. Leontsinis[1,2,a] and K. Ntekas[1,2,b]
on behalf of the ATLAS Muon Collaboration

[1] *National Technical University of Athens*
[2] *Brookhaven National Laboratory*

Abstract. The ATLAS collaboration has chosen the Micromegas technology along with the small-strip Thin Gap Chambers for the upgrade of the inner muon station in the high-rapidity region, the so called New Small Wheel upgrade project. It will employ eight layers of Micromegas and eight layers of small-strip Thin Gap Chambers per wheel. The New Small Wheel project requires fully efficient Micromegas chambers, able to cope with the maximum expected rate of 15 kHz/cm^2 featuring single plane spatial resolution better than 100 μm. The Micromegas detectors will cover a total active area of $\sim 1200\,\mathrm{m}^2$ and will be operated in a moderate magnetic field (≤ 0.3 T). Moreover, together with their precise tracking capability the New Small Wheel Micromegas chambers will contribute to the ATLAS Level-1 trigger system. Several studies have been performed on small ($10 \times 10\,\mathrm{cm}^2$) and medium ($1 \times 0.5\,\mathrm{m}^2$) size prototypes using medium ($1 - 5\,\mathrm{GeV/c}$) and high momentum ($120 - 150\,\mathrm{GeV/c}$) hadron beams at CERN. A brief overview of the results obtained is presented.

ATL-MUON-PROC-2015-013
19 November 2015

1 Introduction

The upgrade of the Large Hadron Collider (LHC) at CERN foresees a luminosity increase by a factor 5. To cope with the corresponding rate increase, the ATLAS detector [1] needs to be upgraded. The upgrade will proceed in two steps: Phase-I in the LHC shutdown 2018/19 [2] and Phase-II in 2023-25 [3]. For the ATLAS Muon Spectrometer the largest Phase-I upgrade concerns the replacement of the two first muon stations, called Small Wheels (SW), in the high-rapidity region with a New Small Wheel system (NSW) [4]. The NSW is expected to cope with the highest rates expected after Phase-II and enhance the performance of the forward muon system by adding trigger functionality to the first muon station.

The NSW employs eight layers of Micromegas detectors (MM) and eight layers of small-strip Thin Gap Chambers (sTGC) [5]. Both technologies will provide tracking and triggering information, resulting into a fully redundant system. Each of the two wheels will consist of sixteen sectors divided into eight large and eight small sectors according to their size. A graphical representation of one

[a] e-mail: Stefanos.Leontsinis@cern.ch
[b] e-mail: Konstantinos.Ntekas@cern.ch

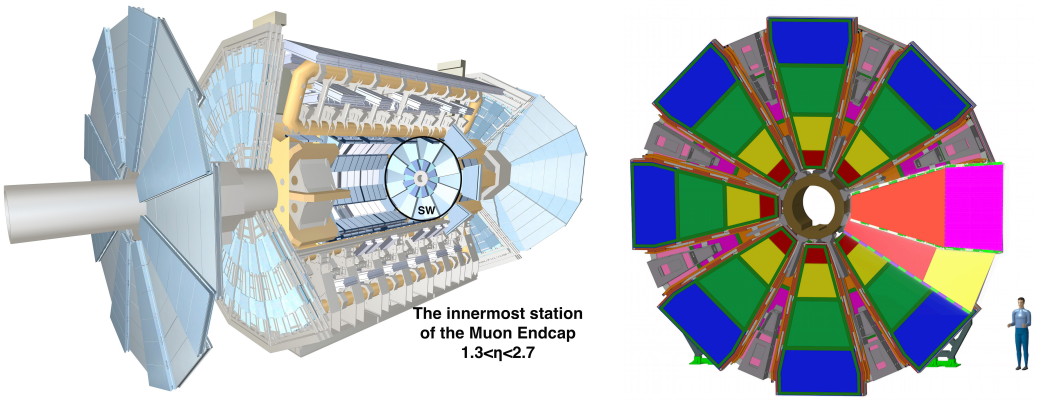

Figure 1. Left: The muon system of the ATLAS experiment. The SW region corresponds to the innermost muon endcap region. Right: Graphical representation of an assembled NSW. Two micromegas sectors, one small and one large, are also shown. Actually the MM will not be visible sitting in between the 2 sTGC quadruplets as shown in Fig. 2.

NSW is shown in Fig. 1 (right). The two technologies will be combined in four wedges per sector following the sTGC-MM-MM-sTGC configuration as shown in Fig. 2. A wedge is a quadruplet combining four layers of the same detector technology.

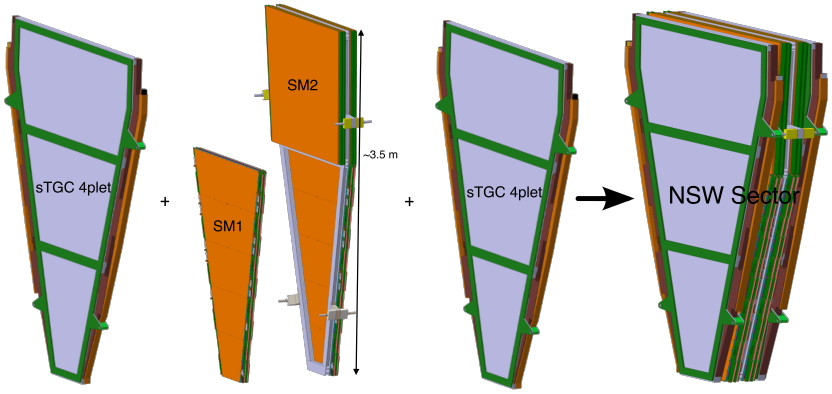

Figure 2. Combining the four MM wedges (quadruplets) into a NSW small sector. The MM detectors will be placed in between the two sTGC quadruplets. The two different types of small MM modules (SM1 and SM2) along with the size of the MM sector in the radial direction are shown.

The main characteristics of the resistive MM detector technology along with performance studies of small chambers in test beams are presented in the following sections. The results demonstrate the excellent performance of the MM chambers that fulfil the requirements of the NSW project in terms of hit reconstruction accuracy and efficiency. A brief description of the reconstruction techniques that

have been developed to take full advantage of the fine intrinsic detector spatial resolution is also given followed by detailed investigation of the small efficiency losses that are measured and are attributed to the internal structure of the detector.

2 The resistive strip MM detector

The MM technology was developed in the middle 1990's introducing a micropattern gaseous detector with two asymmetric regions [6]. Standard MM detectors consist of a planar (drift) electrode, a a few millimetres thick gas gap acting as conversion and drift region, and a thin metallic mesh placed at $\sim 100 - 150\,\mu$m distance from the readout electrode, creating the amplification region. The HV potentials are chosen such that the electric field in the drift region is a few hundred V/cm, and $40 - 50\,$kV/cm in the amplification region achieving gas gain values of the order of 10^4 for the commonly used Ar+7%CO_2 gas mixture. The large multiplication factor is essential for the detection of minimum ionising particles with high efficiency.

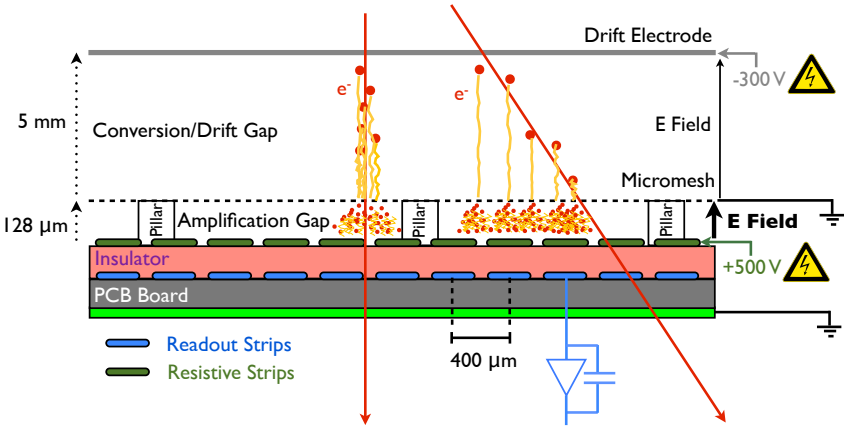

Figure 3. Cross-section of the resistive MM internal structure. A layer of resistive strips matching the read-out pattern makes the detector insensitive to discharges coming from massive ionisations.

Charged particles traversing the drift space ionize the gas molecules and the electrons, liberated by the ionization process, drift towards the mesh (in tens of nanoseconds). With an electric field in the amplification region $\sim 50 - 100$ times stronger than the drift field, the mesh is transparent to more than 95 % of the electrons. The electron avalanche takes place in the thin amplification region in about a nanosecond, resulting in a fast pulse on the readout strip [7]. The ions that are produced during the avalanche process move towards the mesh with velocities about 200 times smaller than the electrons producing also a signal, though smaller, on the readout strips. The drifting of the electrons and the avalanche formation in the amplification region, for perpendicular and inclined tracks, are illustrated in Fig. 3.

In the case of highly ionizing particles the Raether limit [8] may be reached and discharges (sparks) start to occur. Sparks may damage the detector structure or the readout electronics and lead to large dead times as a result of high voltage breakdown. By adding a layer of resistive strips on top of a thin

insulator directly above the readout electrode, as shown in Fig. 3, the MM becomes spark-insensitive. The readout electrode is no longer directly exposed to the charge created in the amplification region. The signal is induced on the resistive strips and then capacitively coupled to the readout strips. By adding the resistive protection some fraction of the signal amplitude is lost but the chamber can be operated at higher gas gain because sparking is reduced by about three orders of magnitude and the effect is only locally constrained in a small region of the detector [9]. Hence, resistive MM chambers can be efficiently operated in a high-rate environment as was demonstrated by testing small resistive prototypes inside the ATLAS experiment with particle rates up to 80 kHz/cm^2 [10, 11].

3 Performance studies

3.1 Test beam activities

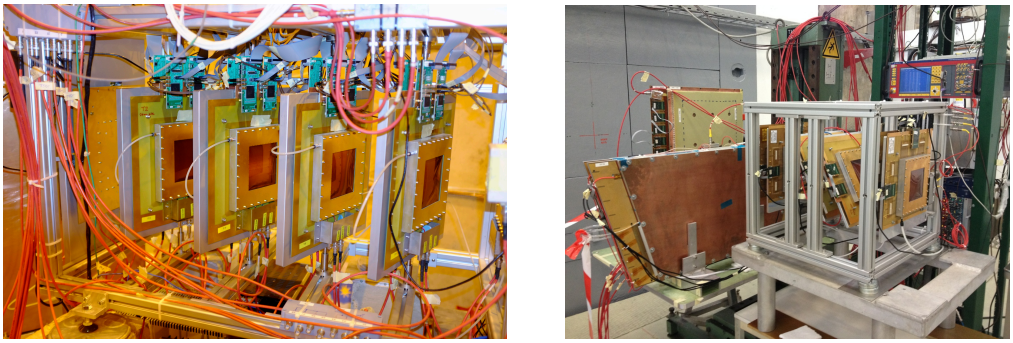

Figure 4. Photos from test beam periods at CERN (SPS H6 and PS T9 respectively). Left: A hodoscope of 8 small ($10 \times 10\,\mathrm{cm}^2$) resistive MM were exposed to a high momentum ($120 - 150\,\mathrm{GeV/c}$) π^+ beam during the summer of 2012. Right: The same hodoscope along with medium size prototypes were tested in a medium momentum ($5 - 10\,\mathrm{GeV/c}$) p beam during the summer of 2014.

In order to demonstrate the excellent performance of the MM technology and also to optimise the design and operational parameters of the detector several resistive MM chambers have been tested with medium/high energy hadron beams. Photographs from two of the experimental set-ups are shown in Fig. 4. For the results that are presented here the front-end electronics were based on the APV25 ASIC (128 channels) [12], which will not be employed in the NSW, readout through the Scalable Readout System (SRS) developed by the RD51 collaboration [13]. The front-end ASIC providing the trigger and tracking primitives for both the MM and sTGC of the NSW will be the VMM [14] currently being produced in its second prototype version. Extensive studies of the first version of the VMM using small resistive MM chambers are reported in [15, 16].

3.2 Hit & track reconstruction techniques

One of the most attractive characteristics of the MM technology is its excellent spatial resolution due to the fine readout segmentation. Moreover, because of the asymmetric field configuration and the large multiplication in the amplification region, the chambers are sensitive to a single primary ionisation electron. Using the time evolution of the integrated charge per channel, sampled every 25 ns by the APV25 chip, the arrival time of each electron is measured along with the total charge,

allowing the detector to work as TPC allowing for precise reconstruction of track segments with a single detector plane. Using the recorded charge and time information, two different hit reconstruction techniques have been developed:

- **(Charge) Centroid :** Average of the strip position weighted by the strip charge.
- **μTPC** : 2D track reconstruction transforming the arrival time into distance. The hit is defined as the interpolation of the track in the middle of the drift gap. The track angle is also measured using the slope of the reconstructed segment.

The charge centroid method reconstructs hits with high accuracy when the particle traverses the chamber plane perpendicularly. In this case, the charge is shared among a few strips allowing for a very precise charge interpolation. The spatial resolution obtained with this method is well below 100 μm for perpendicular tracks. The μTPC method does not provide accurate results in this case as the pulse in each strip is the aggregation of pulses induced by more than one primary ionisation cluster generated at different times. When the particle crosses the detector under an angle the signal induced in each strip is most probably coming from one primary cluster with several strips fired from a single track. In this occasion, the μTPC method provides a very accurate measurement of the particle hit position on the detector. In the case of inclined tracks, owing to the distribution of the primary ionisation clusters along several readout strips, the strip signal amplitude becomes sensitive to the primary cluster charge fluctuations. As a consequence, the accuracy of the charge centroid method deteriorates with increasing track inclination angles and it cannot be used for non-perpendicular tracks.

The hit positions reconstructed with the centroid and μTPC methods can also be integrated in a combined hit per gas gap. The combination algorithm weights the contribution of each of the two hits (centroid and μTPC) with the size of the track footprint [17]. In the case of large clusters the μTPC method contributes more while in clusters with a size smaller than four strips the combined hit is primarily defined by the centroid method. The combined point provides a single plane hit reconstruction with a resolution better than 100 μm independently of the track incident angle [18].

3.3 Refinement of the μTPC method

The performance of the μTPC track reconstruction method is of great importance for the MM community and also for the ATLAS NSW upgrade project where the particle track angles expected are between 8 and 30°. One of the issues that were studied was the refinement of the clustering algorithm to properly treat events with more than one track, or events with noise and/or delta rays ($\sim$ 10% of the events). A pattern recognition technique, using the Hough transform, has been developed which filters out the real tracks increasing the efficiency of the event selection and improving the accuracy of the reconstructed track by removing outlying strips [16].

Moreover, due to the readout/resistive elements geometry, there is a non-negligible capacitance between the strips causing the ionisation charge to be shared among the neighbouring strips. The effect has been extensively studied in simulation concluding that $\sim$ 10% of the charge induced on a strip is capacitively coupled to its neighbours[1]. This may bias the reconstructed track by artificially increasing the cluster size in cases where the strips on the edges of the cluster have signal coming only from the coupling with their neighbours. A filtering algorithm has been developed identifying

[1]The effect depends on the strip pitch and width. For this study a geometry with strips 300 μm wide separated by a gap of 100 μm was used.

such hits and discarding them from the track reconstruction procedure.

Another parameter that should be treated carefully is the assignment of the hit position with respect to the strip pitch. In the offline reconstruction each hit position is usually assigned in the middle of the strip pitch. In fact, this is correct only for the middle strips of the cluster where the hit position is uniformly distributed along the strip pitch. For the edges of the cluster it is more probable for the hit position to be towards the strip pitch edge neighbouring to the cluster strips. The assignment of the hit in the middle of the strip pitch for the cluster edges results in biasing the reconstructed track towards larger inclination values, thus a method has been developed tuning the hit position on the cluster edges based on their charge [19].

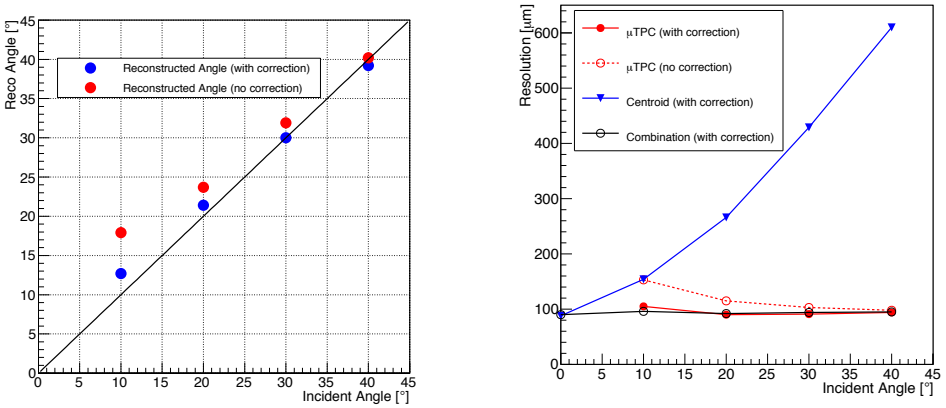

Figure 5. Left: The reconstructed incident track angle, peak value of the angular distribution, versus the true inclination angle before (red points) and after the correction (blue points). Right: The spatial resolution along the different incident angles measured before and after the correction with the μTPC (red circles) and the centroid (blue triangles) methods. The resolution measured when combining the two methods, after the correction, is also shown (black circles) [20] .

The refined μTPC reconstruction algorithm was applied in data taken during July 2012 test beam at CERN where small size ($10 \times 10\,\mathrm{cm}^2$) chambers were exposed to a $120\,\mathrm{GeV/c}$ π^+ beam and results with and without the new recipe are compared. The improvement in the accuracy of the μTPC method, using the techniques described above, is not only evident in the better agreement of the measured incident angle with the true one shown in Fig. 5 (left), but also in the measurement of the spatial resolution which is displayed in Fig. 5 (right). The impact of the correction is more significant for smaller incident angle values where a 30% improvement in the measured spatial resolution is achieved. The results for the combined point are also shown with the black line on the right plot of Fig. 5. The spatial resolution of the combined point has been measured to be better than 100 μm for inclination angles $0° - 40°$.

3.4 Efficiency studies

In addition to the precise hit position reconstruction the NSW MM detectors should be fully efficient even at the highest rates of $15\,\mathrm{kHz/cm}^2$ that are expected after the LHC upgrade. In this direction the

efficiency of the small MM chambers has been studied in test beams in order to fully characterize and understand possible contributions to the detector inefficiency. Results for chambers with different characteristics and with different track inclination angles are presented.

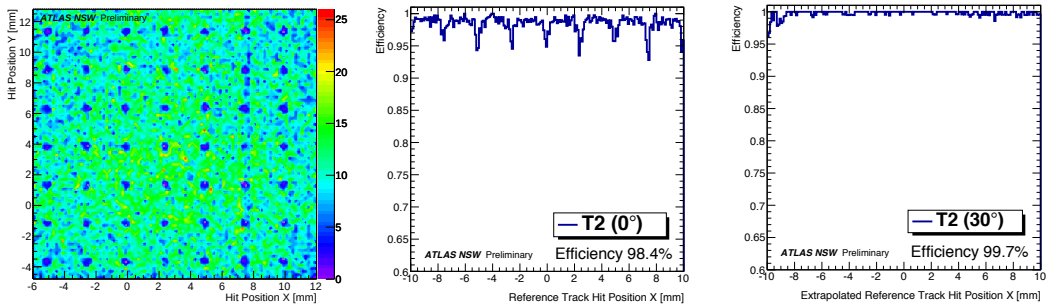

Figure 6. Left: The 2-D distribution of the hit positions measured in a MM with two-dimensional readout reveals the inefficient areas of the chamber corresponding to the pillars that define the width of the amplification region. Middle: Using a reference track the efficiency is plotted as a function of the extrapolated reference hit position on the chamber plane. A geometrical inefficiency of 1.6%, owing to the pillars, is measured along a 2 cm region for perpendicular tracks. Right: In the case of tracks inclined by 30° the efficiency becomes insensitive to the pillars ($\sim$ 100%) as several strips are fired by a single charged particle [20].

By using a MM with two-dimensional readout the profile of the beam can be directly obtained by reconstructing the centroid hit in the two coordinates. The resulting distribution obtained for perpendicular tracks is shown in Fig. 6 (left). Only a small rectangular area of the detector is shown ($18 \times 18\,\mathrm{mm}^2$) corresponding to the central area of the beam with the highest statistics. The histogram population increases by going from the blue coloured areas to the green ones. Several inefficient spots can be distinguished on the two dimensional maps corresponding to the cylindrical pillar structure appearing every 2.5 mm.

By comparing the hits reconstructed in a single chamber with the reference chambers of the experimental set-up a measurement of the efficiency can also be performed. The measured efficiency is plotted as a function of the reference track hit position for a resistive MM chamber with a single readout layer in Fig. 6 (middle, right). In the middle, the case where the chamber plane is positioned vertically with respect to the beam axis is shown. Local efficiency drops, by 5%, owing to the pillars appear every 2.5 mm. The total measured efficiency is rather high with only $\sim$ 1.6% geometrical inefficiency attributed to the pillars. If however the chamber is inclined by 30° with respect to the beam the pillars are no longer visible as shown in Fig. 6 (right). The larger track footprint for inclined tracks makes the efficiency measurement insensitive pillars and a perfect efficiency is reached.

4 Conclusions

After an intensive R&D phase, which begun in 2007, the MM technology has evolved significantly over the last years and it was finally approved as one of the technologies that will be used in the NSW upgrade project of the ATLAS experiment. This is the first application of a Micropattern Gaseous

Detector (MPGD) technology in a very large scale experiment and in a high rate environment. A series of performance studies is ongoing in order to optimise the detector performance and operating conditions. Being the primary precision tracker of the NSW efforts are mainly focussed in the development of the μTPC reconstruction method allowing for a precise segment reconstruction using a single detector gap. Moreover, a single plane hit reconstruction accuracy better than 100 μm independently of the track angle has been achieved by combining different reconstruction techniques. A very high efficiency has been measured for the MM chambers tested in test beams at CERN. The 1.6% geometrical inefficiency coming from the pillar structure supporting the mesh is evident only for the perpendicular tracks. For larger inclination angles, like the track angles expected in the NSW ($8^\circ - 30^\circ$), the efficiency remains unaffected by the pillars reaching $\sim 100\%$ values.

Acknowledgements

This research has been co-financed by the European Union (European Social Fund - ESF) and Greek national funds through the Operational Program "Education and Lifelong Learning" of the National Strategic Reference Framework (NSRF) - Research Funding Program: **THALES**. Investing in knowledge society through the European Social Fund.

References

[1] ATLAS Collaboration, JINST 3 S08003 (2008).
[2] ATLAS Collaboration, CERN-LHCC-2011-012, LHCC-I-020 (2011).
[3] ATLAS Collaboration, CERN-LHCC-2012-022, LHCC-I-023 (2012).
[4] ATLAS Collaboration, CERN-LHCC-2013-006, ATLAS-TDR-020 (2013).
[5] V. Smakhtin *et al.*, Nucl. Instr. Meth. A 598 196-200 (2009).
[6] Y. Giomataris *et al.* , Nucl. Instr. Meth. A376, 29-35, (1996).
[7] I. Giomataris *et al.* , Nucl.Instrum.Meth. A560, 405-408, (2006).
[8] H. Raether, Z. Phys., 112 (1939), p. 464
[9] T. Alexopoulos *et al.*, Nucl. Instr. Meth. A 640 110-118 (2011).
[10] T. Alexopoulos *et al.*, ATL-MUON-PUB-2013-002 (2013).
[11] Y. Kataoka *et al.*, JINST 9 C03016 (2014).
[12] M.J. French *et al.*, Nucl. Instr. Meth. A466, 359-365, (2001).
[13] S. Martoiu *et al.*, Nucl. Sc. Symp. and Med. Imag. Conf., IEEE, pp.2036,2038 (2011).
[14] G. De Geronimo *et al.*, IEEE Transactions on Nuclear Science, vol. 60, no. 3, (2013).
[15] G. Iakovidis, CERN-THESIS-2014-148 (2014).
[16] T. Alexopoulos *et al.*, ATL-UPGRADE-PUB-2014-001 (2014)
[17] C. Bini, JINST 9, C02032 (2014)
[18] S. Leontsinis, CERN-THESIS-2015-077 (2015).
[19] K Ntekas, ATL-MUON-PROC-2014-011 (2014)
[20] ATLAS NSW Public Results : https://twiki.cern.ch/twiki/bin/view/AtlasPublic/NSWPublicResults